Exp Brain Res (2006) 168: 11–24
DOI 10.1007/s00221-005-0069-z

RESEARCH ARTICLE

Sara Johansson · Ann-Cathrin Radesäter
Richard F. Cowburn · Johan Thyberg · Johan Luthman

Modelling of amyloid β-peptide induced lesions using roller-drum incubation of hippocampal slice cultures from neonatal rats

Received: 17 February 2005 / Accepted: 12 May 2005 / Published online: 21 September 2005

Abstract Pronounced neurodegeneration of hippocampal pyramidal neurons has been shown in Alzheimer's disease. The aim of this study was to establish an organotypic in vitro model for investigating effects of the amyloid β (Aβ)-peptide on pyramidal neuron degeneration, glial cell activation and tau phosphorylation. Tissue cultures in a quasi-monolayer were obtained using roller-drum incubation of hippocampal slices from neonatal Sprague Dawley rats. Neuronal populations identified included *N*-methyl-D-aspartate (NMDA-R1) receptor immunoreactive pyramidal neurons, and neurons immunopositive for glutamic acid decarboxylase-65 (GAD65) or gamma amino butyric acid (GABA). Many neurons expressed phosphorylated tau as shown by pS^{396}, AD2 and PHF-tau immunostaining. Astrocytes, microglial cells and macrophages were also identified. The A$\beta_{25–35}$ peptide formed fibrillar networks within 2 days as demonstrated by electron microscopy. In the presence of the neurotoxic A$\beta_{25–35}$ peptide, but not A$\beta_{35–25}$, deposits developed in the tissue that were stainable with Thioflavine T and Congo red and showed the characteristic birefringence of Aβ plaques. Following A$\beta_{25–35}$ exposure, neurodegenerative cells were observed with Fluoro-Jade B staining. Further characterization of pyramidal neurons immunopositive for NMDA-R1 showed a decrease of cell number in the immediate surrounding of A$\beta_{25–35}$ deposits in a time- and concentration-dependent fashion. Similar effects on pyramidal neurons were obtained following exposure to the full-length, A$\beta_{1–40}$ peptide. Also, a loss of neuronal processes was seen with GAD65, but not GABA, immunohistochemistry after exposure to A$\beta_{25–35}$. A$\beta_{25–35}$-exposed neurons immunopositive for phospho-tau showed degenerating, bent and often fragmented processes. Astrocytes showed increased GFAP-positive reactivity after A$\beta_{25–35}$ exposure and formation of large networks of processes. No obvious effect on microglial cells and macrophages could be seen after the A$\beta_{25–35}$ exposure. The developed in vitro system may constitute a useful tool for screening novel drugs against Aβ-induced alterations of tau and degeneration of hippocampal neurons.

Keywords Alzheimer's disease · Neurodegeneration · Organotypic cultures · Pyramidal neurons · Glutamate receptors

S. Johansson (✉) · A.-C. Radesäter · J. Luthman
Local Discovery Research Area CNS & Pain Control,
AstraZeneca, S-151 85 Södertälje, Sweden
E-mail: Sara.Johansson@astrazeneca.com
Tel.: +46-8-55325461
Fax: +46-8-55323840

S. Johansson · R. F. Cowburn
Karolinska Institutet, Neurotec Department,
Division of Experimental Geriatrics, Novum,
S-14186 Huddinge, Sweden

J. Thyberg
Karolinska Institutet, Department of Cell and Molecular Biology,
Medical Nobel Institute, Stockholm, Sweden

Introduction

The key neurohistopathological features of Alzheimer's disease (AD) are the extracellular accumulation of amyloid deposits as well as the intracellular aggregation of hyperphosphorylated tau protein in the form of neurofibrillary tangles (NFTs). In addition to these pathologies there is extensive synaptic degeneration and neuronal cell loss (Glenner and Wong 1984; Grundke-Iqbal et al. 1986). The brain regions most affected in AD include the hippocampus, enthorhinal cortex, amygdala, neocortex and certain basal forebrain nuclei (Braak and Braak 1994). Pyramidal glutamatergic hippocampal neurons seem to be especially vulnerable in AD and are affected early in the pathological process (Bobinski et al. 1998). Amyloid β (Aβ)-peptide, a 39–43 amino acid proteolytic product of the amyloid precursor protein (APP) (Selkoe et al. 1996), is the main component of the mature senile plaques found in AD. Amyloid accumulates in cerebrovascular deposits and in various plaque

structures. Classical senile/neuritic plaques consist of a central amorphous core, which can be identified by histological stains such as Congo red (Klunk et al. 1989) and Thioflavine T (Sage et al. 1983) and show a characteristic "apple green" birefringence under polarized light. The senile plaques are spherical and enclosed by dystrophic neurites (Glenner 1989), reactive astrocytes (Pike et al. 1995a) and microglia (Bamberger and Landreth 2002; Perlmutter et al. 1990). In particular, microglia are thought to contribute to neuronal cell death in AD by releasing neurotoxins (Giulian et al. 1996), such as nitric oxide, in response to Aβ-stimulation (Casal et al. 2002). Several synthetic Aβ-peptides, including the shorter A$\beta_{25–35}$ peptide, have been shown to be directly toxic to cell lines (Doig et al. 2002) and to primary neuronal cell cultures (Abe and Saito 2000).

Tau is the principal component of paired helical filaments (PHF), which are in turn the main constituent of NFTs. NFTs are found within the neuronal perikaryon as well as within neuropil threads and dystrophic neurites surrounding senile plaques. NFTs are composed of hyperphosphorylated forms of the microtubule-associated tau protein (Grundke-Iqbal et al. 1986). In AD, hyperphosphorylated tau aggregates into paired helical filaments (PHFs) in the cytoplasm of degenerating neurons. PHF-tau is hyperphosphorylated at several serine and threonine sites (Hanger et al. 1998) that can be studied using antibodies such as AD2 and AT8. AD2 (or PHF-1) recognizes tau phosphorylated at Ser396 and 404 (Otvos et al. 1994; Buee-Scherrer et al. 1996), whereas AT8, recognizes PHF-tau phosphorylated at both Ser202 and Thr205 (Goedert et al. 1993, 1995).

Pathophysiological processes implicated in AD can be studied in various in vitro systems, such as cell lines (Misonou et al. 2000), primary cultures (Zheng et al. 2002) and organotypic slice cultures (Harrigan et al. 1995). The roller-drum technique of slice cultures yields thin cultures that present certain advantages over other in vitro systems. Slice cultures of hippocampus retain important anatomical features and much of the synaptic organization of the intact tissue (Gähwiler 1981). Individual cells in roller-drum cultures can be viewed with phase-contrast microscopes, the cultures are easily manipulated and diffusion barriers for exogenously applied substances are limited as compared to resting cultures of the Stoppini type (Stoppini et al. 1991). Also long-term culturing permits recovery from dissection trauma and allows adaptation to the in vitro environment. Due to the flattening of the cultures to a quasi-monolayer, and their growth on glass coverslips, roller-drum cultures are ideally suited for experiments that require microscopical analysis. The disadvantages of this culture system, compared to resting cultures, include a lower degree of cellular organization and a partial loss of a distinct brain anatomy. The present study characterizes and evaluates roller-drum hippocampal slice cultures as a system for studying the consequences of Aβ-exposure on neuronal and glial cell populations and on the phosphorylation state of the tau protein.

Materials and methods

Roller-drum hippocampal cultures

Roller-drum cultures of hippocampus were prepared essentially according to Gähwiler (Gähwiler 1981), with modifications described by Luthman et al. (1998). Three to five-day-old postnatal Sprague Dawley rat pups were killed by decapitation and their brains removed under sterile conditions. The hippocampus was dissected out, placed in Gey's balanced salt solution (GBSS) and thereafter cut into 250 μm thick slices with a tissue chopper (Mc Illwain, USA). The slices were transferred to a petri dish containing 2 ml of GBSS and only intact hippocampal slices containing the CA1–CA3 and dentate gyrus were selected under a light microscope. The tissues were then attached to sterile 12×24 mm glass cover slips (No.1; Gribi, Switzerland) with a mixture of reconstituted chicken plasma (Sigma) and thrombin (1000 NIH units; Sigma) in the proportions 1:2; thrombin:chicken plasma. After coagulation for 30 min at room temperature, the cover slips were transferred to sterile plastic tubes (Falcon) containing 1.0 ml of medium. The medium (100 ml) consist of 56.0 ml Dulbecco's modified Eagle's medium with glutamine (Gibco), 32.5 ml Hank's balanced salt solution (Gibco), 0.66 ml of a 45% glucose solution (Sigma), 1.0 ml of a 1 M HEPES solution (Gibco) and 10 ml heat-inactivated fetal bovine serum (HyClone). 1% antibiotic-antimycotic solution (Sigma) containing penicillin, streptomycin and amphotericin B was added to the medium until the first medium change. The cultures were grown at 37°C/ 5% CO_2, placed in a roller-drum tilted at 5° to the horizontal axis, and rotated at 60 revolutions per hour exposing the cultures to gaseous or water phases every minute. Medium was changed every 2 days. Fresh medium was prepared every week. After 3 weeks in vitro, A$\beta_{25–35}$, A$\beta_{35–25}$ or A$\beta_{1–40}$ dispersed in distilled water was added to the medium at a final concentration of 50 μM. Control cultures were grown in parallel with the Aβ-cultures, with fresh medium changed every other day. Medium was changed once (day 2) during the four day Aβ exposure. Each culture set included 100–120 roller-drum cultures that were prepared from 6 to 7 rat pups. Treatment- (A$\beta_{25–35}$) and control groups each contained 50–60 cultures that were randomly allocated to the different groups without any prior evaluation of culture condition. A few slices were lost during the culturing period, meaning that the final groups consisted of 40–50 cultures. Each treatment group (control and A$\beta_{25–35}$) were then randomly divided into groups consisting of 15–20 cultures that were stained with the different primary antibodies as described above.

The animal experimental procedure followed the provisions and general recommendations of Swedish animal protection legislation, and was approved by the South Stockholm Committee for Ethical Experiments on Laboratory Animals (license S28/01).

Exposure of hippocampal slice cultures to $A\beta_{25-35}$ and $A\beta_{35-25}$

$A\beta_{25-35}$ and $A\beta_{35-25}$ peptides used in these experiments were purchased from Bachem. The peptides were freshly dispersed in distilled water at a concentration of 1 mg peptide/ml dH_2O (stock solution) and diluted in culture medium at a final concentration of 50 μM for application to the cultures. All cultures used in these experiments had been kept for 3 weeks in vitro at the time the peptides were added. Also $A\beta_{1-40}$ (Bachem) was dispersed in water, diluted directly in culture medium and added to the cultures.

Electron Microscopy

$A\beta_{25-35}$ was dispersed in distilled water at a concentration of 1 mg/ml and centrifuged at 1000 g for 2 min to remove possible non-dissolved material (stock solution). Further dilution was then made in culture medium to a final concentration of 50 μM. Samples were taken for electron microscopy (EM) after incubation for either 2 or 48 h at 37°C in a humidified atmosphere of 5% CO_2 in air (tissue culture conditions). The incubated solutions were centrifuged at 20,000 g for 20 min to sediment aggregated material. This material was then suspended in 100 μl of water by gentle sonication and 5 μl aliquots were placed on grids covered by a carbon-stabilized formvar film. After 2 min, excess fluid was removed with a filter paper, and the grids were negatively stained with 2% uranyl acetate in water. The specimens were finally examined and photographed in a Jeol EM 100CX at 60 kV.

Immunohistochemistry

After treatment, slice explants on coverslips were fixed with 0.4% formaldehyde (Apoteket) and 0.125% glutaraldehyde (Sigma) in 0.1 M PBS (pH 7.4) for 30 min and then washed several times with PBS. Incubation with a 10% methanol solution containing 3% hydrogen peroxide was used to quench endogenous peroxidase activity. Cultures were blocked for 1 h in 1% BSA, washed in PBS, and incubated with the appropriate primary antibody, diluted in PBS containing 0.3% Triton X-100 (Sigma) and 0.5% normal serum (goat or horse; Vector), for 72 h at + 4°C. Hippocampal neurons were identified with antibodies against the NMDA receptor glutamate ion channel receptor subunit, NMDA-R1 (monoclonal mouse IgG, PharMingen; diluted 1:600, 72 h incubation), glutamic acid decarboxylase 65, GAD65 (monoclonal mouse IgG2a, anti-glutamic acid decarboxylase, clone GAD-6, Sigma; diluted 1:200, 72 h incubation) and gamma aminobutyric acid, GABA (polyclonal rabbit IgG; Sigma; diluted 1:10 000, 72 h incubation). The different tau-antibodies used included: pS396 (polyclonal rabbit phosphospecific anti-tau, Biosource; diluted 1:250, 72 h incubation, AD2 (monoclonal murine IG1 anti-human phosphorylated tau protein, Bio-rad; diluted 1:5000, 72 h incubation) and AT8 (monoclonal mouse anti-human PHF-tau, Innogenetics; diluted 1:250, 72 h incubation). Other antibodies used included those against glial fibrillary acidic protein (GFAP; monoclonal mouse IgG 1, Sigma; diluted 1:100, 24–72 h incubation), and the antibodies ED1 (mouse anti rat IgG, Serotec; diluted 1:1000, 72 h incubation) and CD11b (mouse anti rat IgG, clone MRC OX-42, Serotec; diluted 1:200 and 1:500, 72 h incubation) against microglial cells and macrophages. After the incubation, cultures were washed in PBS and incubated with the biotinylated secondary antibody (ABC-Elite Vectastain kit, Vector; diluted 1:200, 30 min incubation). The cultures were washed with PBS, incubated with the avidin–biotin complex (Vector) for 1 h and visualized by the chromogen DAB reaction with diaminobenzidine tetrahydrochloride (1 mg/ml; FAST^{TM} DAB Tablet Set; Sigma). In GABA-immunostained cultures, the GFAP antibody was used for verification and characterization of the GABA-positive astrocytes. The binding of the GFAP antibody was visualized using a nickel-intensified DAB protocol (Vector), leading to a black/violet staining of astrocytic processes. Finally, after the reaction, cultures were dehydrated in ethanol, cleared in xylene, and mounted with Eukitt (VWR International). Non-specific staining was defined by exclusion of the primary antibody in the staining procedure.

Thioflavine T, Congo red and Fluoro-Jade B-staining

The light microscopic characteristics of the $A\beta_{25-35}$ aggregates were studied using Thioflavine T staining (Sage et al. 1983) and the alkaline Congo red technique (Klunk et al. 1989) according to established procedures. To detect degenerating neurons the cultures were stained with the fluorochrome Fluoro-Jade B and examined with a fluorescence microscope using an FITC filter. Fluoro-Jade B is an anionic fluorochrome that can be used for histological staining of neurons undergoing degeneration (Schmued et al. 1997). The fixed cultures were first immersed in a solution containing 1% sodium hydroxide in 80% ethanol for 5 min, followed by 2 min in 70% ethanol and 2 min in dH_2O. The cultures were then transferred to a solution of 0.06% potassium permanganate for 10 min on a shaker table. After rinsing in dH_2O for 2 min the cultures were placed in the staining solution containing 0.0004% Fluoro-Jade B in 0.1% acetic acid for 20 min. After rinsing 3×3 min in dH_2O the cultures were dried, cleared in xylene and mounted with DPX.

Microscopical observation and image documentation

The sections were analyzed by light microscopy at a primary magnification of 10–40× (LEICA DMLB). Pictures were taken with a digital camera (Kappa PS30; Kappaopto-electronicsGmbH) at either 20× or 40× magnifications. The camera was connected to a standard

desktop computer with a software (Migra, Euromed Networks AB, Stockholm) in which the light-/darkness and colour balance were adjusted. Brightness and contrast of the image were further adjusted using Adobe Photoshop 6.0. Fluorescence pictures were taken at 20× or 40× magnification with a digital camera (Hamamatsu, Hamamatsu Photonics Norden AB, Sweden) connected to a fluorescence microscope (Nicon Eclipse E600).

Quantification of the number of cells and Aβ-plaque numbers

Under light microscopy, the total number of NMDA-R1 receptor subunit immunoreactive cells showing neuronal pyramidal morphology was counted in each culture. Also neurons positive for GAD 65 and GABA and the number of Congo red stained plaques were counted in Aβ-exposed and control cultures. No Congo red staining could be seen in the controls. The results are presented as mean values ± standard error of the mean (SEM) or standard deviation (SD).

Statistical analysis

Results are expressed as means ± standard error of the mean (SEM) or standard deviation (SD). Statistical analyses were performed with one-way or two-way ANOVA, followed by Bonferroni-Dunn's post-hoc testing (GraphPad Prism ver 4.0).

Results

General appearance of hippocampal slice cultures

After three weeks in vitro, the mature hippocampal slice cultures had flattened and consisted of a thin and elongated mantle of cells in a quasi monolayer. The size of the tissue and the cellular density varied somewhat between the cultures.

Aggregation of synthetic A$\beta_{25–35}$

Immediately after the addition of 50 μM A$\beta_{25–35}$ to the culture medium, EM identified aggregated material of a largely amorphous character. The aggregates varied in size but did not show any clear organized structure at this time. Following 2 h of incubation at 37°C, small assemblies of short fibrillar fragments and flake-like structures were observed (Fig. 1A). Two days (48 h) after addition of A$\beta_{25–35}$ to the medium, large aggregates consisting of a network of amyloid fibrils were identified (Fig. 1B). In the Aβ exposed cultures, aggregates were identified that showed positive staining for both Thioflavine T (Fig. 2A) and Congo red (Fig. 2C and D). These aggregates varied in shape and size (compare Fig. 2C and D) and when stained with Congo red produced a characteristic "apple green" birefringence using polarized light microscopy (Fig. 2E). The Congo red stained plaques present in the A$\beta_{25–35}$-exposed cultures were counted under the light microscope in a few slides. The number of deposits ranged from 177 to 226 per culture, but the considerable variability in their size and shape precluded any detailed estimates of the extent of amyloid deposition.

The effect of A$\beta_{25–35}$ on cell viability

Fluoro-Jade B was used to stain degenerating neurons in the cultures. In control cultures almost no or a very faint staining of neurons could be seen (Fig. 3A), while after exposure to A$\beta_{25–35}$ for 4 days, several stained neurons were seen (Fig. 3B). The Fluoro-Jade B stained neurons showed a round and condensed appearance following A$\beta_{25–35}$ exposure.

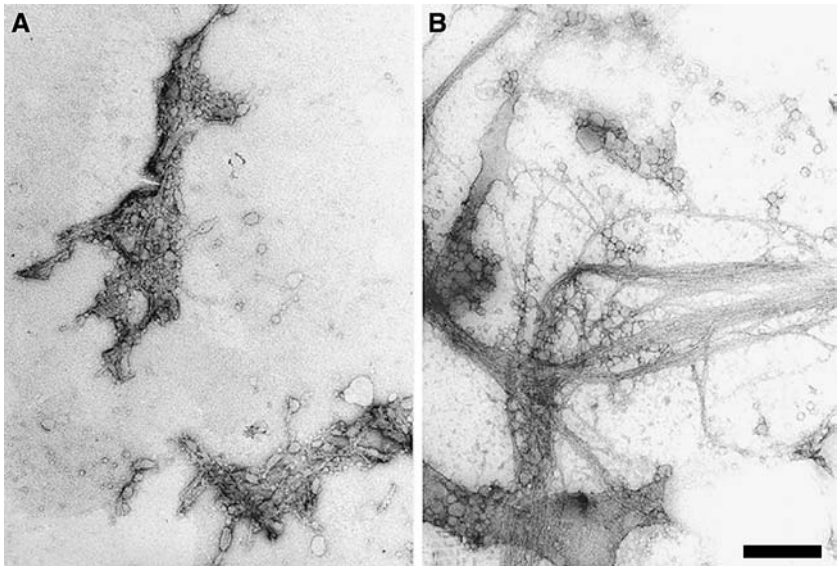

Fig. 1 Electron micrographs of A$\beta_{25–35}$ aggregation. A$\beta_{25–35}$ was dispersed in distilled water, diluted in culture medium to a final concentration of 50 μM, incubated at 37°C in a CO_2-incubator, and processed for EM as described in Methods. **A** Aggregates of short fibrillar fragments and flake-like structures formed after 2 h incubation. **B** Networks of amyloid fibrils formed after 2 days of incubation. Scale bar = 200 nm

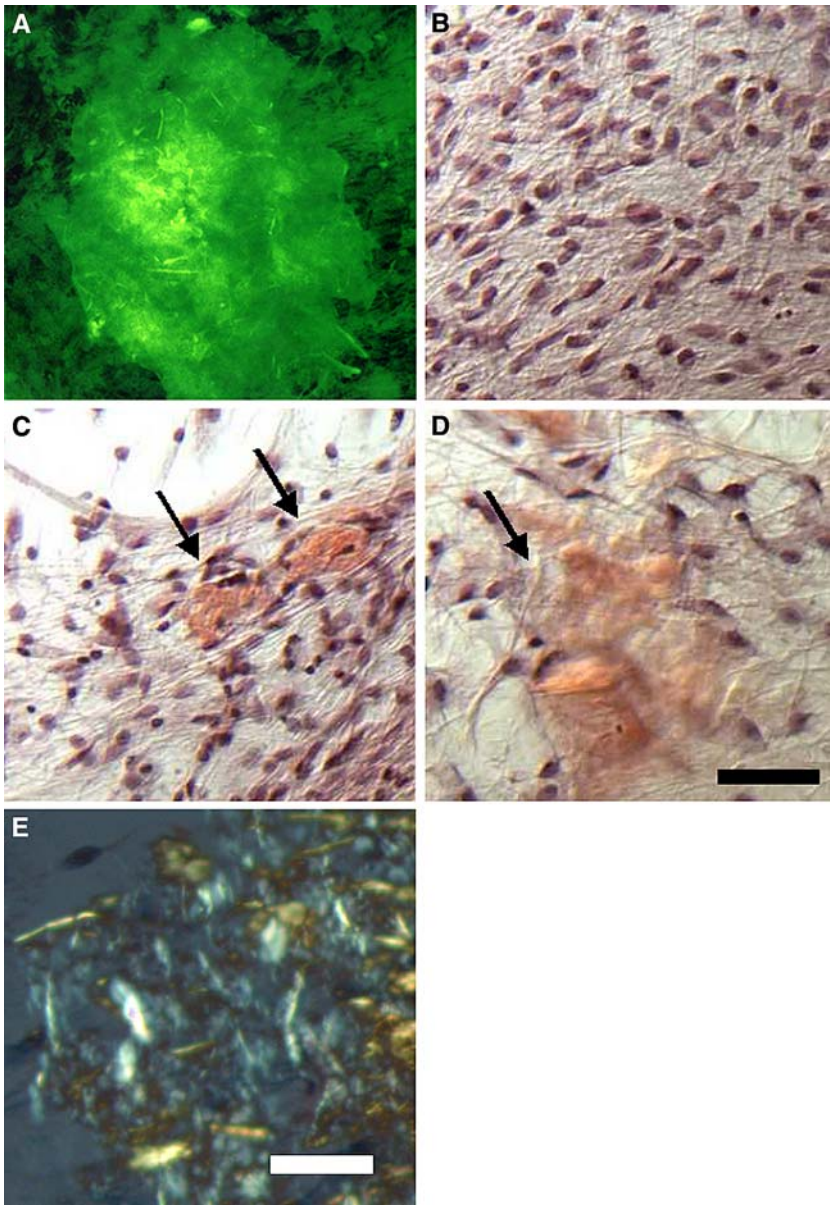

Fig. 2 Fibrillar aggregates formed after Aβ_{25-35} exposure for 4 days in slice cultures from rat hippocampus grown for 3 weeks in a roller-drum system. **A** Amyloid aggregates stained with Thioflavine T. **B** Control culture grown for 21 days and stained with Congo red. **C** and **D** Aβ_{25-35} exposed cultures with aggregates stained with Congo red (arrows). (E) Amyloid aggregates expressing green birefringence under polarized light in an Aβ_{25-35} exposed culture stained with Congo red. **B**–**D** images generated using Nomarski optics. Scale bar **B**–**D** = 50 μm, *E* = 100 μm

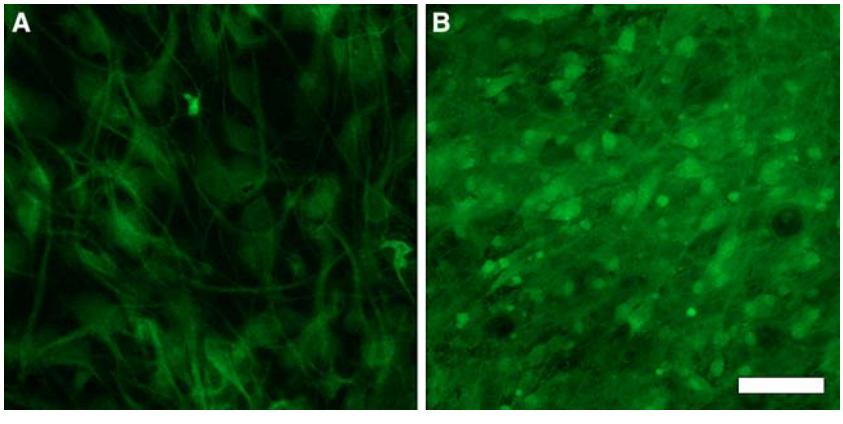

Fig. 3 Fluoro-Jade B-staining in slice cultures from rat hippocampus grown for 3 weeks in a roller-drum system. **A** Fluoro-Jade B-stained control culture. **B** Fluoro-Jade B-stained Aβ_{25-35} exposed culture. Scale bar = 50 μm

NMDA-R1 immunoreactive pyramidal neurons and effect of A$\beta_{25–35}$ exposure

NMDA-R1 immunostaining showed numerous labelled cells in the slice cultures that were organized in identifiable rows with varying degree of cellular layering (Fig. 4A). At higher magnification, medium to large sized NMDA-R1 immunostained neurons were observed that showed a pyramidal morphology with long and well developed processes (Fig. 4C). The neurons typically occurred either in groups or in rows. The NMDA-R1-immunoreactivity appeared to be localized throughout the cytoplasm of both the perikarya and cellular processes. Cultures exposed to 50 μM A$\beta_{25–35}$ for 4 days showed a clear loss of the number of NMDA-R1 immunostained neurons, concomitant with the occurrence of deposits that could be visualized with the NMDA-R1 staining alone (Fig. 4B). Double staining of the slides with Congo red showed that the NMDA-R1 positive deposits overlapped with structures positive for Congo red (inserted picture in Fig. 4D). The cultures exposed to A$\beta_{25–35}$ showed both a decreased number of NMDA-R1 cells and a loss of stained processes. Several NMDA-R1 immunostained cells with no processes at all and a round cell body were commonly seen around the Aβ deposits (Fig. 4D–F). Cultures exposed to the

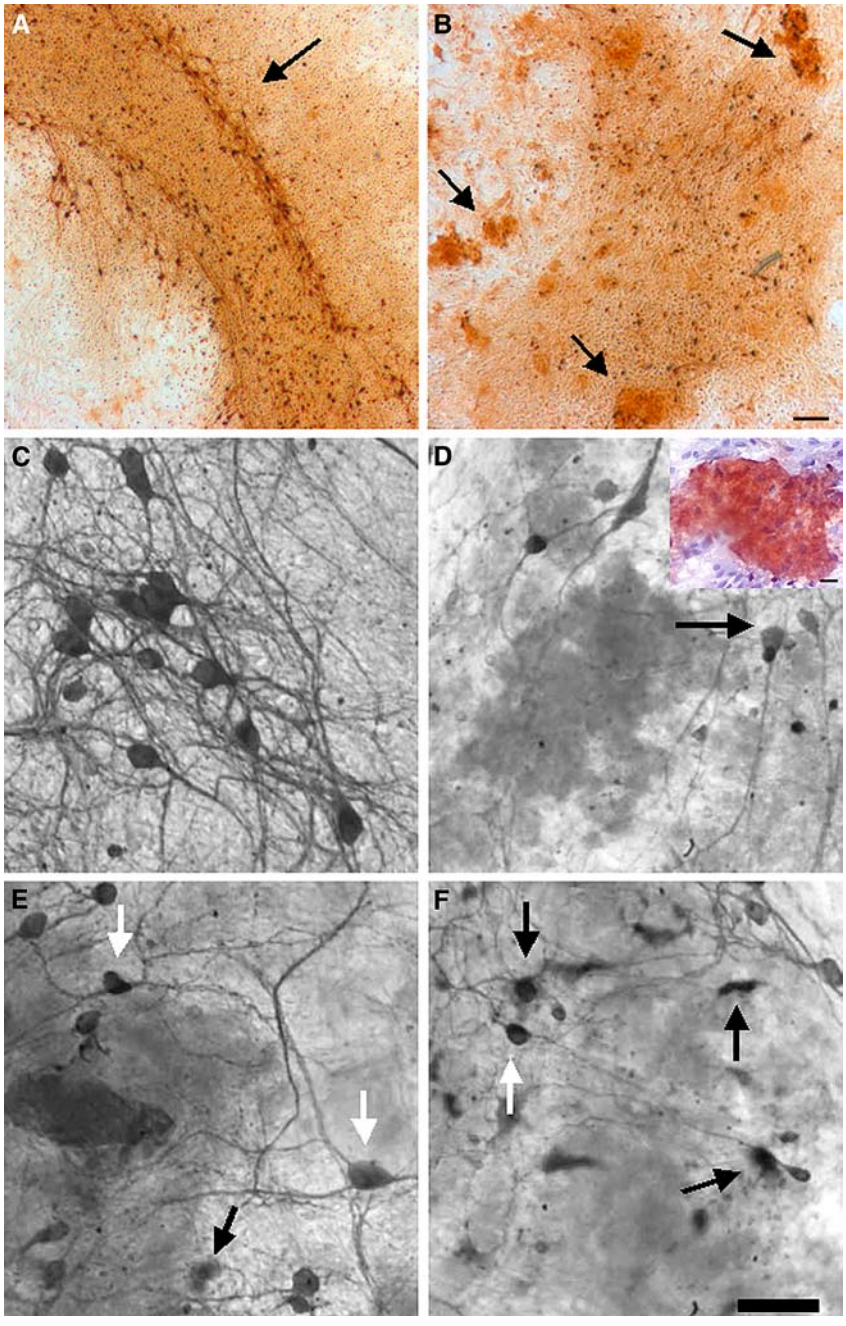

Fig. 4 NMDA-R1-immunoreactive neurons in slice cultures from rat hippocampus grown for 3 weeks in a roller-drum system. At low magnification NMDA-R1-immunoreactive cells in a control culture are seen occurring in rows **A** (arrow), while in a culture exposed to 50 μM A$\beta_{25–35}$for 4 days there is a substantial reduction in the number of stained cells concomitant with the occurrence of labelled deposits **B** (arrows). **C** The NMDA-R1-immunoreactive cells in a control culture are medium to large pyramidal-shaped neurons with well-developed and extended processes. **D–F** Cultures exposed to A$\beta_{25–35}$ lead to a marked loss of the neurons and a decreased number of processes in the remaining cells. Around the Aβ deposits, most cells have rounded cell bodies and only few processes (black arrows). A few cells appear to be unaffected by the Aβ exposure even in close association to the deposits (white arrows). The inserted picture in D shows Congo red staining of a NMDA-R1 labelled A$\beta_{25–35}$-deposit. Images generated using Bright field optics. Scale bar **A–B** = 250 μm, **C–F** = 50 μm

$A\beta_{35–25}$ reversed sequence peptide did not show any morphological changes of the neurons (Fig. 5B).

Concentration and time effects of synthetic $A\beta_{25–35}$ on pyramidal neurons

A concentration dependency of the $A\beta_{25–35}$-induced loss of NMDA-R1 stained cells was shown after 4 days exposure to 1, 30 and 50 μM $A\beta_{25–35}$. There was an approximately 60% loss at the 50 μM concentration (Fig. 6A). One-way ANOVA indicated a significant concentration-effect of $A\beta_{25–35}$ $F(6,42) = 3.054$. Post-hoc testing (Bonferroni) demonstrated that the 50 μM concentration significantly decreased the number of NMDA-R1 positive cells ($P < 0.05$). The time-dependency was studied by exposing the cultures for 6 h, 1, 2, 3 and 4 days with 50 μM $A\beta_{25–35}$. Two-way ANOVA indicated a significant Group-effect, $F(1,90) = 16.98$ and a significant Time-effect, $F(4,90) = 6.13$. Post-hoc testing demonstrated that 4 days exposure of $A\beta_{25–35}$ produced a significant effect on the number of NMDA-R1 positive cells ($P < 0.05$), as shown in Fig. 6B. Also, $A\beta_{1–40}$ was used in one set of experiments to compare the neurotoxic action of $A\beta_{25–35}$ with that due to full-length $A\beta_{1–40}$ peptide. The loss of NMDA-R1 labelled pyramidal neurons was observed at 50 μM $A\beta_{1–40}$ and was similar to the neurotoxicity seen with 50 μM $A\beta_{25–35}$. Moreover, deposits of $A\beta_{1–40}$ peptide were detected in the tissue using the NMDA-R1 antibody in a similar fashion to that seen after $A\beta_{25–35}$ exposure (data not shown).

GAD 65 and GABA immunoreactive interneurons and the effect of $A\beta_{25–35}$

To detect GABA-ergic interneurons in the cultures we used 2 antibodies; anti-GAD 65 and anti-GABA. Both GAD 65 and GABA immunoreactive neurons with extended processes were found throughout the tissue (Fig. 7A–D). The GABA staining was broader, staining both neurons and astrocytes (confirmed by GFAP-staining), while the GAD 65 antibody seemed to be more specific and only stained neurons. The GAD 65 antibody

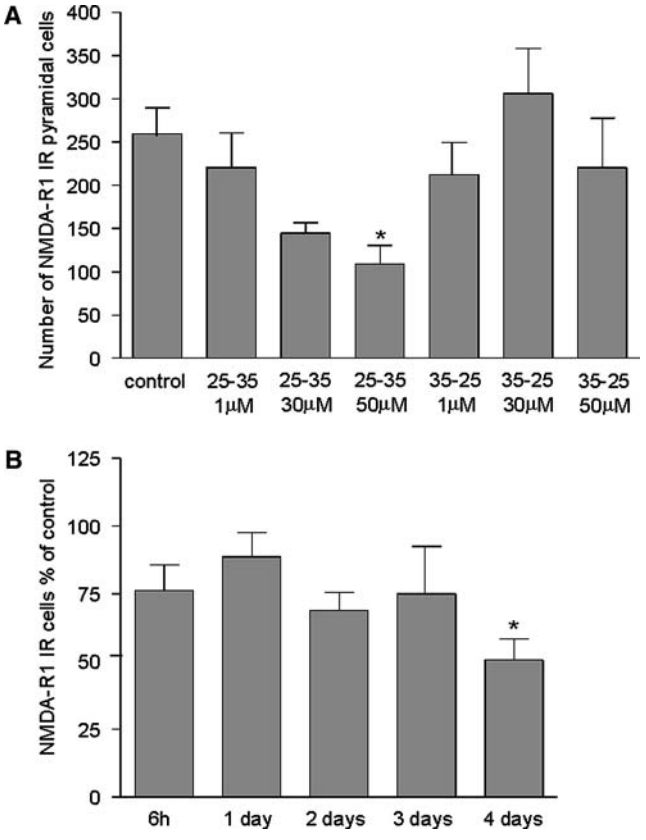

Fig. 6 Concentration and time dependency of $A\beta_{25–35}$ on number of NMDA-R1 stained cells. **A** Hippocampal slice cultures from rats were exposed to 1, 30 and 50 μM $A\beta_{25–35}$ for 4 days. 50 μM $A\beta_{25–35}$ demonstrated the largest effect, with a cell loss of ~60%. The reversed peptide, $A\beta_{35–25}$, had no effect on the number of pyramidal neurons. Pyramidal neurons were identified using immunostaining of the NMDA-R1 receptor subunit and all immunopositive cells in each culture were counted. Data is expressed as mean of NMDA-R1 positive cells ±SEM. One-way ANOVA, followed by Bonferroni-Dunn's post-hoc test; * $P < 0.05$. **B** Hippocampal slice cultures from rats were exposed to 50 μM $A\beta_{25–35}$ for 6 h, 1 day, 2 days, 3 days and 4 days. Pyramidal neurons were identified using immunostaining of the NMDA-R1 receptor subunit. The largest cell loss (~50%) was found following 4 days exposure to 50 μM $A\beta_{25–35}$. The effect of each time point is expressed as per cent of the respective control group ±SEM (SEM control groups varied between 5%–13%). Two-way ANOVA, followed by Bonferroni-Dunn's post-hoc test; * $P < 0.05$

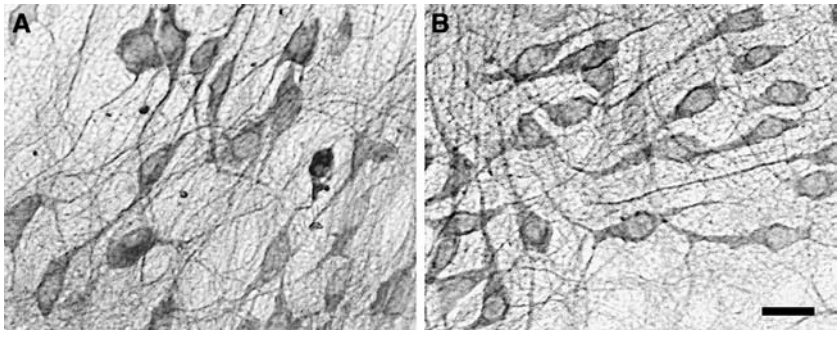

Fig. 5 NMDA-R1-immunoreactive neurons in slice cultures from rat hippocampus grown for 3 weeks in a roller-drum system and exposed to 50 μM $A\beta_{35–25}$ (reversed $A\beta_{25–35}$ peptide) for 4 days. No detectable toxic effect on the neurons can be observed after the $A\beta_{35–25}$ exposure **B** as compared to control cultures **A**. Images generated using Bright field optics. Scale bar = 25 μm

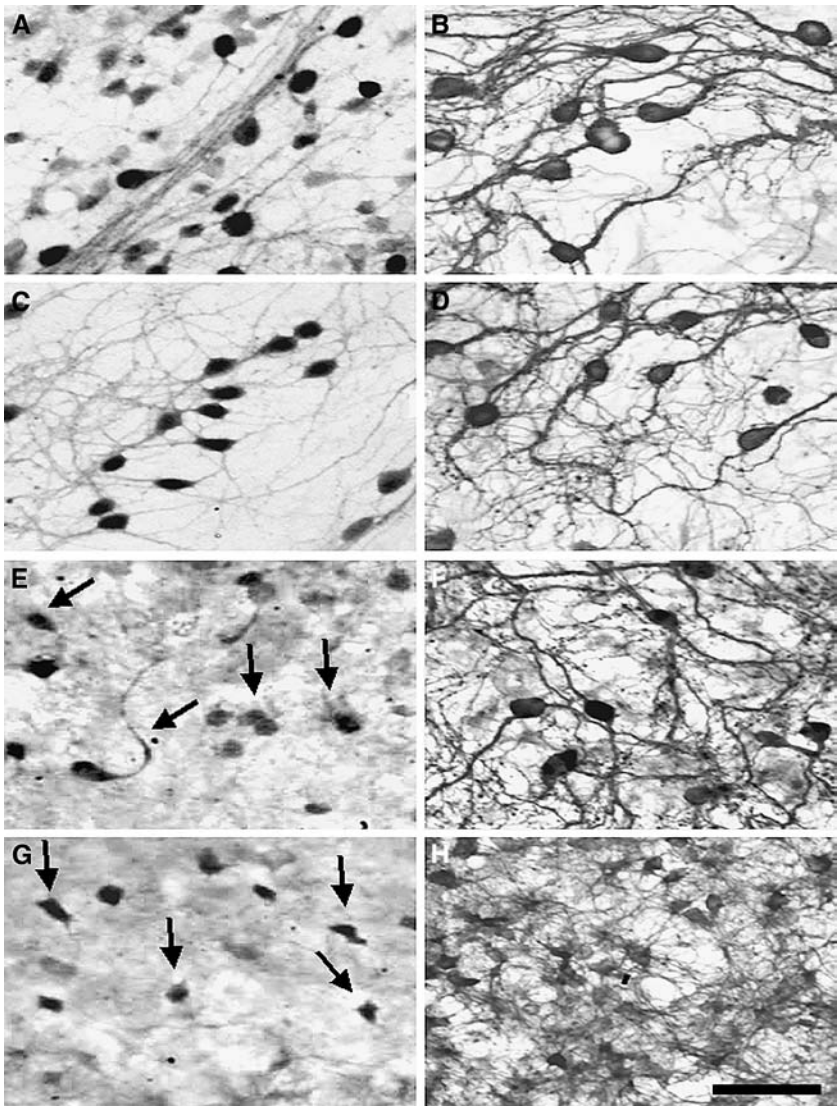

Fig. 7 **A** and **C** GAD 65- and **B** and **D** GABA-immunoreactive interneurons in control slice cultures from rat hippocampus grown for 3 weeks in a roller-drum system. Extensive neuronal networks of GAD 65- and GABA immunopositive neurons are found throughout the tissue. The neurons are mostly seen at the border of the tissue. **E** and **G** GAD 65 immunoreactive neurons in Aβ_{25-35} exposed cultures have few or no processes (arrows). **F** GABA immunoreactive neurons appear to be unaffected after Aβ_{25-35} exposure with an intact network of processes. **H** GABA immunopositive astrocytes are changed into a more reactive phenotype following Aβ_{25-35} exposure. Large networks of astrocytes have developed and cover the whole tissue. Images generated using Bright field optics. Scale bar = 50 μm

detected large networks of interneurons (Fig. 7A and C) but the number of GAD 65 positive neurons in the cultures appeared to be fewer than GABA positive neurons. To confirm this observation, GAD 65- and GABA-immunoreactive neurons in control- and Aβ_{25-35} exposed cultures were counted under the light microscope. No effect of Aβ_{25-35} on the number of GABA-positive cells could be seen. The mean numbers ($\pm$SD) of GABA-immunoreactive neurons in control and Aβ_{25-35}-treated cultures were 283 ± 61 and 319 ± 88, respectively ($n = 15$ cultures). In contrast, the number of GAD 65 positive neurons appeared to be decreased in Aβ_{25-35}-treated cultures (from 181 ± 46 to 71 ± 41, $n = 15$). Following Aβ_{25-35} exposure for 4 days the number of GAD 65 positive neurons was decreased and the remaining cells had few or no processes. In some Aβ-exposed cultures, GAD 65 positive neurons with few or no processes were seen (Fig. 7E), while in others the tissue was almost devoid of GAD 65 positive cells (Fig. 7G). The GABA-positive neurons appeared to be more resistant to Aβ exposure (Fig. 7F), on the other hand GABA immunopositive astrocytes appeared to have a more reactive phenotype following Aβ exposure and large networks of astrocytes developed covering the whole tissue (Fig. 7H). With GFAP-staining we could demonstrate that these GABA-positive processes formed after the Aβ-exposure were astrocytic (Fig. 9D).

Tau immunoreactive neurons and the effect of Aβ_{25-35}

The mAbs Ser396 and AD2 were used to stain cells for phosphorylated tau at epitopes Ser396 and Ser396/Ser404 (Otvos et al. 1994). The mAb AT8, which recognizes a phosphate-dependent epitope at Ser202/Thr205, was used for detecting PHF tau in cells (Goedert et al. 1995). Control cultures contained networks of neurons, with long processes, positive for the AT8, pS396 and AD2 antibodies (Fig. 8A, C, E). After 4 days of Aβ_{25-35} exposure, several tau-immunoreactive neurons with few or no processes were observed. The cell bodies showed a round appearance, and the processes

appeared to be degenerating, bent, curly and sometimes fragmented (Fig. 8B, D, F).

The effect of Aβ_{25-35} on astrocytes, microglia and macrophages

Numerous large GFAP immunostained astrocytes were found throughout the tissue in control cultures (Fig. 9A). Networks of astrocyte processes developed after 4 days exposure to Aβ_{25-35} (Fig. 9B). Figure 9B (insert) shows a GFAP-stained Aβ-exposed culture that is also stained with Congo red, indicating that the plaques were often surrounded by several astrocytes. Co-staining with GFAP of a GABA-stained control culture showed few GFAP positive astrocytic processes (Fig. 9C), whereas after Aβ_{25-35}-exposure large networks of astrocytic processes immunopositive for GFAP were seen (Fig. 9D). This indicates that the GABA-positive astrocytic processes that we observed following Aβ_{25-35} (Fig. 7H) were also GFAP-positive. Microglial cells and macrophages, as identified with the antibodies ED1 and OX42, were also seen in the cultures (Fig. 10). Although a few ED1 and OX42 immunoreactive cells showed a more reactive morphology following 4 days exposure to Aβ_{25-35}, this effect was not generally obvious (Fig. 10C–F). Neither the number nor the morphology of microglial cells appeared to be changed appreciably after Aβ exposure.

Discussion

Roller-drum hippocampal slice cultures exposed to the Aβ peptide 25–35 fragment were evaluated as a histopathology model of AD. In roller-drum cultures, the

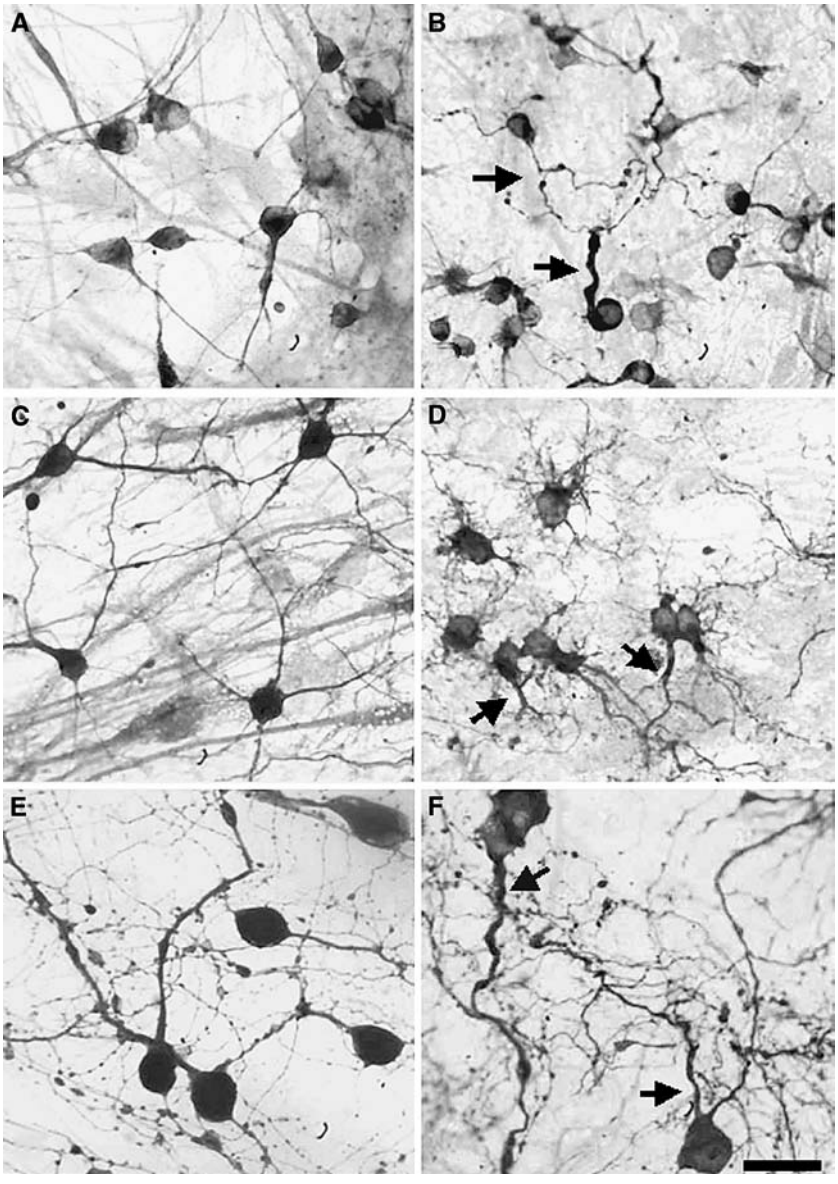

Fig. 8 Immunohistochemical detection of tau immunoreactive neurons in slice cultures from rat hippocampus grown for 3 weeks in a roller-drum system. **A** Staining of PHF tau with AT8 mAb in a control culture showing neurons with extended processes. **C** and **E** Neurons immunoreactive for pS396 and AD2, respectively, in control cultures. **B**, **D** and **F** Neurons stained with AT8, pS396 and AD2 in cultures exposed to Aβ_{25-35}. Cell bodies are rounded and cell processes appear to be degenerated with a bent, curly and sometimes fragmented appearance (arrows). Images generated using Bright field optics. Scale bar = 25 μm

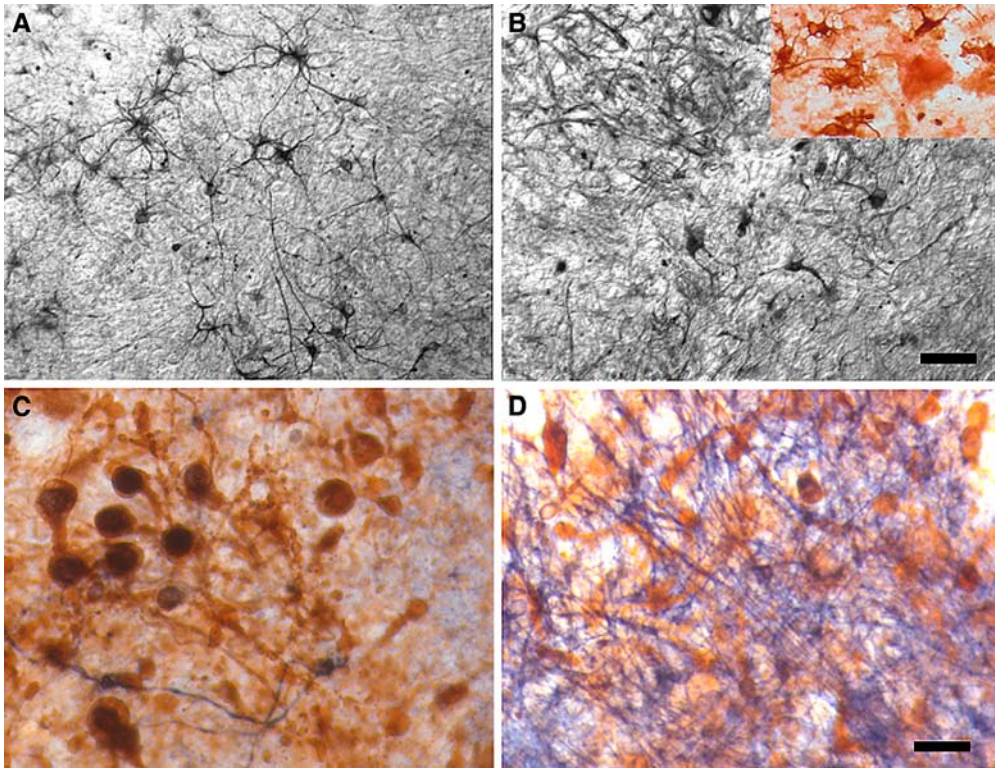

Fig. 9 Immunohistochemical detection of astrocytes in rat hippocampal slice cultures grown in a roller-drum system for 3 weeks. **A** In a control culture, a GFAP-positive network of astrocytes is identified throughout the tissue. **B** After exposure to A$\beta_{25–35}$, a large network of astrocyte processes, covering the whole tissue is seen. The cell bodies are hard to distinguish due to the fibrillar network that has developed after A$\beta_{25–35}$ exposure. The inserted picture shows a Congo red stained GFAP-immunopositive culture. The plaques are often surrounded by several astrocytes following A$\beta_{25–35}$-exposure. **C** A GABA-stained control culture, co-stained with GFAP. **D** A GABA-stained A$\beta_{25–35}$-exposed culture, co-stained with GFAP. Following A$\beta_{25–35}$-exposure, a large network of GABA-immunopositive astrocytic processes developed that also was positive for GFAP **D**. Images generated using Bright field optics. Scale bar **A**–**B** and **C**–**D** = 50 μm

tissue is embedded in a plasma clot on coverslips and thereafter incubated under slow rotation, causing a continuous changing of the liquid-gas interface (Gähwiler 1981). The major advantage with this technique is that a quasi-monolayer develops, while phenotypically advanced cell populations are maintained. The final thickness of the slices after weeks of culturing is the major difference between the most common slice culture techniques (e.g. roller-drum cultures and membrane cultures). Due to the flattening of the cultures to a quasi-monolayer, and their growth on glass coverslips, roller-drum cultures are easily studied using a regular light microscope, without the need for sectioning of the tissue. Indeed hippocampal neurons in such cultures have been shown to retain many of their in vivo properties (Zim mer and Gähwiler 1984). A disadvantage with roller-drum cultures is that the characteristic cytoarchitecture of the tissue of origin is only partially preserved. After weeks in culture, the slice has spread out over the coverslip resulting in a disorganization of the tissue compared to the in situ architecture. In membrane cultures on the other hand, the culture is at rest (no movement). This appears to keep the culture in a more "fixed" state and the organotypic structure is better preserved.

Using the neurotoxic A$\beta_{25–35}$ fragment of Aβ (Yankner et al. 1990; Pike et al. 1993, 1995b), we examined if neuronal and glial cells were changed either morphologically or in number. After mixing the A$\beta_{25–35}$ peptide in culture medium, highly fibrillar networks developed within 2 days. Previous studies have shown that both A$\beta_{25–35}$ and A$\beta_{1–42}$ form stable aggregates, even when diluted in medium (Pike et al. 1991). A$\beta_{25–35}$ aggregates exhibit positive Thioflavine T staining, a histological property characteristic both for Aβ aggregates in vitro (LeVine 1993) and senile/neuritic plaques in vivo (Klunk et al. 2001). These observations suggest that A$\beta_{25–35}$ shares important properties with full length Aβ peptides. Indeed, our A$\beta_{25–35}$ treated cultures showed deposits that were positive for the amyloid stains Thioflavine T and Congo red and expressed the classical green birefringence with Congo red staining under polarized light, suggesting β-pleated sheet formation. The neurotoxic effect of A$\beta_{25–35}$ on NMDA-R1 labelled pyramidal cells was also compared to the effect of A$\beta_{1–40}$. The result of this comparison suggested that the neurotoxic actions of A$\beta_{25–35}$ and A$\beta_{1–40}$ were very similar in the slice cultures, and that similar deposits occurred with either peptide. Organotypic hippocampal

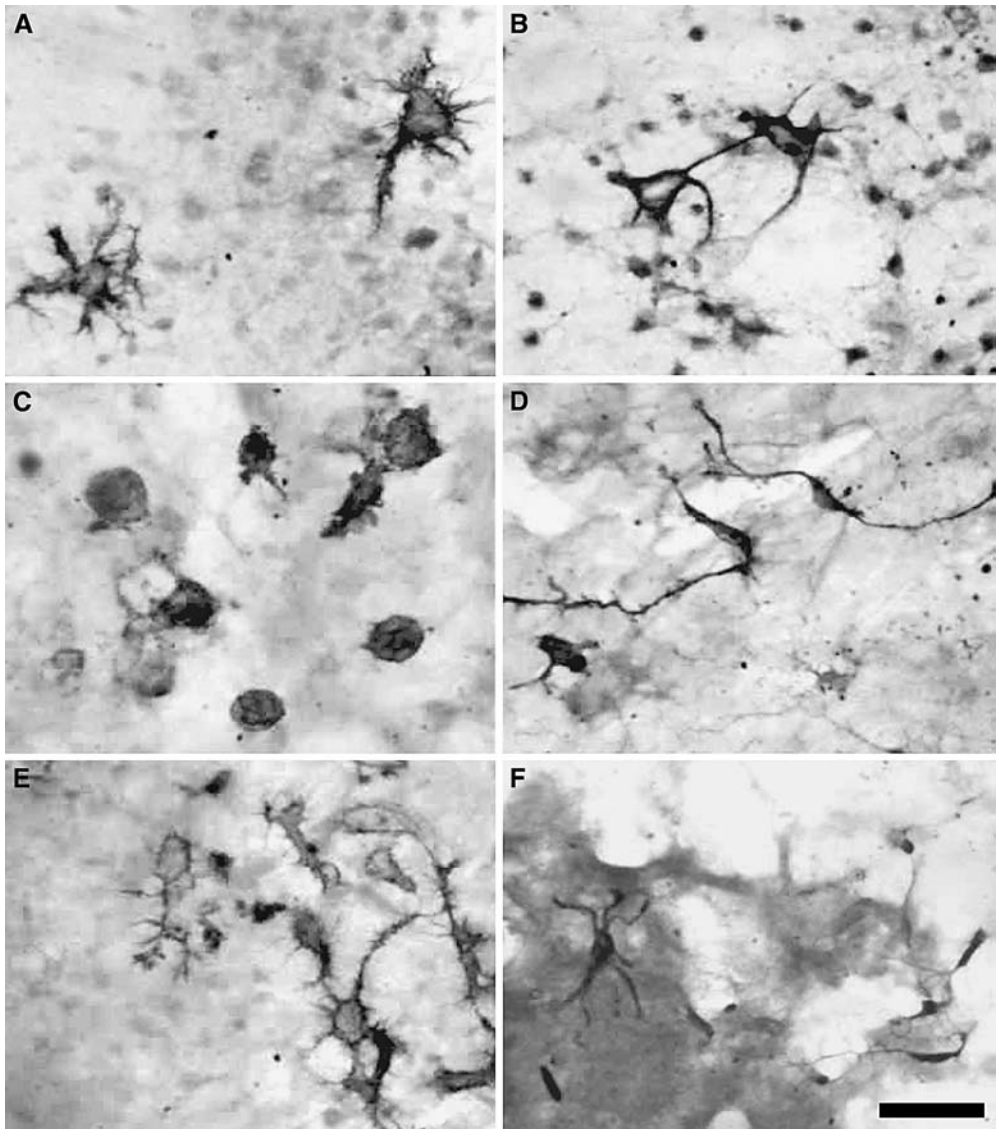

Fig. 10 Immunohistochemical detection of microglial cells and macrophages in hippocampal slice cultures grown for 3 weeks in a roller-drum system. **A** OX42 immunopositive cells in a control culture. **B** Control culture with ED1 immunopositive cells. **C** and **E** OX42 positive cells after exposure to Aβ_{25-35}. **D** and **F** ED1 positive cells after exposure to Aβ_{25-35}. Images generated using Bright field optics. Scale bar = 50 μm

slice cultures have been used to study effects of both Aβ_{25-35} and Aβ_{1-40}. When injected into area CA3 of hippocampal slices cultured on membranes, Aβ_{1-40} was shown to produce degenerating somata and pyknotic nuclei following injection (Harrigan et al. 1995). Also, cell death has been seen in freshly prepared hippocampal slices pre-soaked in 50 μM Aβ_{25-35} solution and thereafter kept as roller-drum or membrane cultures (Allen et al. 1995). In contrast to this finding and those presented here, Malouf reported that neurons in roller-drum hippocampal slice cultures are insensitive to 100 μM Aβ_{25-35}- and Aβ_{1-28}-exposure for 2–6 days (Malouf 1992). Neither a difference in propidium iodide-labelling of dead cells nor in dendritic length of pyramidal neurons could be observed in control and Aβ-exposed cultures. Furthermore, granule cells in the dentate gyrus and pyramidal cells in areas CA1 and CA3 remained intact. In our monolayer hippocampal slice cultures we investigated the actions of Aβ_{25-35} on different neuron and glial populations. Neurodegeneration was observed after the Aβ exposure using the neurodegeneration-marker Fluoro-Jade B. Fluoro-Jade B has greater affinity for neurons than its predecessor Fluoro-Jade (Schmued and Hopkins 2000). Both markers have an affinity for the entire neuron including cell body, dendrites, axon and axon terminals. Although this implies that Aβ_{25-35}-exposure caused neurodegeneration, we cannot say which type of cell death occurred. To elucidate which type of cell death arises following Aβ, a technique such as TUNEL-staining is needed to detect apoptotic cells. During culturing, a continuous detachment of dying cells from the cultures limits the possibility to perform a careful examination of the ratio of degenerating cells undergoing various forms of cell death (apoptosis versus necrosis). With Fluoro-Jade B, an increased number of dead neurons could be seen following Aβ-exposure. The results obtained with Fluoro-Jade B, together with the very dramatic decrease

in the number of NMDA-R1 stained pyramidal cells seen following A$\beta_{25–35}$-exposure, provide strong evidence that A$\beta_{25–35}$ induces neurodegeneration in hippocampal roller-drum cultures.

Pyramidal neurons were stained by immunolabeling of the NMDA receptor R1 subunit, whereas interneuron-like cells were identified by GAD 65 or GABA immunostaining. Hippocampal granule and pyramidal cell populations, as well as GABA-ergic interneurons have been identified in hippocampal slice cultures (Beach et al. 1982; Zimmer and Gähwiler 1984). In rat hippocampus, distribution of the NMDA-R1 protein is heterogeneous, with highest expression in pyramidal neurons of the CA1 layer (Toro et al. 2001). In severe Braak and Braak IV–VI staged AD cases, increased NMDA-R1 staining is observed in immunolabeled shrunken and/or dystrophic neurons within CA fields (Braak and Braak 1994), whereas dendrites of NMDA-R1-positive CA3-1 pyramidal neurons display a ''corkscrew'' morphology (Ikonomovic et al. 1999). This is in line with our hippocampal slice culture model, where we found that the NMDA-R1 immunoreactive pyramidal cells were highly affected by A$\beta_{25–35}$. A 4 days exposure to 50 μM A$\beta_{25–35}$ was needed to obtain a robust loss of NMDA-R1 cells. Statistical analyses demonstrated time-dependent effects of the peptide that were statistically significant after 4 days exposure. Also a concentration-dependent effect of A$\beta_{25–35}$ was found with significant effects exerted at 50 μM. The reversed sequence A$\beta_{35–25}$-peptide, at 50 μM, did not produce any visual deposits and caused no effect on cell number in the cultures. In these quantitative studies, a fairly high variability was experienced in the NMDA-R1 pyramidal cell counts, ranging at an SEM around 10–20%. The inherent variability of the cell number in the cultures (observed in control cultures) is most likely dependent on intra-experimental conditions, such as tissue preparation and cell survival in the slices. However, the present findings show that with proper sample sizes, both time-course and concentration-dependent data could be established after exposure to A$\beta_{25–35}$, which may allow studies on mechanisms involved in the neurotoxicity caused by the A$\beta_{25–35}$ deposits and possible neuroprotective approaches. Since A$\beta_{25–35}$ peptide deposits could be identified with the NMDA-R1 antibody in the immunostained sections, it was possible to also directly study how Aβ deposits affected neurons. Congo red staining of these NMDA-R1 stained A$\beta_{25–35}$-deposits confirmed the fact that these aggregates really were amyloidogenic. Many pyramidal neurons in close vicinity to the Aβ deposits showed clear-cut neurodegenerative changes, although a small number of neurons seemed less affected, with intact neurites, even when the cells were positioned close to Aβ-deposits. However, no investigation on the relationship between plaque burden and cell loss was performed.

We used two different antibodies to detect GABA-ergic neurons in the cultures, one directed towards the GABA-synthesizing enzyme GAD 65 (Esclapez et al. 1994) and one towards GABA itself. We found that most GABA-ergic interneurons were found in the border of the tissue. In vivo, rat hippocampus shows a uniform distribution of GABA-ergic interneurons within different hippocampal subfields (Sperk et al. 1997). The roller-drum cultures do not retain a distinct hippocampal neuroanatomy after weeks in culture. It is an artificial system and the cytoarchitecture of hippocampus is changed. Therefore, it is not possible in these cultures to clearly distinguish the different hippocampal layers and as a consequence the exact location of GABA-ergic neurons cannot be confirmed. GABA-ergic interneurons have been reported to be either resistant (Pike and Cotman 1993) or vulnerable (Pakaski et al. 1998) to Aβ exposure. In our culture system, both GAD 65 and GABA immunoreactive networks were detected, although GAD 65 staining was more diffuse and not as intense as GABA staining. The GAD 65-positive cells were severely affected following 4 days of A$\beta_{25–35}$ exposure with only a few small and condensed GAD 65-positive cell bodies remaining. In contrast, GABA immunostaining showed regions of neurons with extended processes remaining after Aβ exposure. Thus, the GABA-producing enzyme GAD seems to be more sensitive to the Aβ-exposure, while GABA is protected and is not affected in the same way. Furthermore, GABA-immunoreactivity in astrocytes was increased after exposure to A$\beta_{25–35}$. With GFAP-staining we could demonstrate that these GABA-positive processes formed after the Aβ-exposure were astrocytic (Fig. 9D). This finding is in line with data showing increased GABA immunoreactivity in astrocytes concomitant with enhanced GFAP immunostaining after neurotoxin lesions (Andersson et al. 1994). This suggests that GABA-positive astrocytes may turn into a more reactive phenotype following Aβ exposure.

In the control cultures, neurons were identified that reacted with antibodies that detect tau phosphorylated on S396, S396/S404 and S202/T205. After A$\beta_{25–35}$ exposure, tau-immunoreactive neurons showed neuronal processes that were bent, curly and sometimes fragmented. Many neurons had lost their processes entirely. Differences in tau phosphorylation are observed during development and neurodegeneration, i.e. periods when neuronal structure is subject to profound changes (Burack and Halpain 1996; Combs et al. 1998). The fact that we saw neurons with phosphorylated tau even in controls is probably due to an immaturity of the cultures that are still under development. Another explanation could be a stressful situation caused by the dissection procedure. A number of studies have shown that Aβ-peptides can induce tau phosphorylation in vitro, leading to microtubule destabilization and eventually neuronal death (Busciglio et al. 1995; Takashima et al. 1998). Furthermore, tau-depleted neurons in hippocampal cultures show no signs of degeneration when treated with fibrillar Aβ, suggesting that tau itself plays a key role in the neurodegenerative processes (Rapoport et al. 2002). This fits well with the results of the present

study, where A$\beta_{25–35}$ caused severe neurodegeneration in neurons immunopositive for the different tau-antibodies as evaluated by immunohistochemistry.

In cultures exposed to A$\beta_{25–35}$, GFAP-positive astrocytes showed a changed morphology, including an expansion of their processes. Following A$\beta_{25–35}$-exposure a large network of astrocytic processes developed that were spread out over the culture (Fig. 9B). These processes covered the tissue and the cell bodies were difficult to distinguish from the network of processes (as compared to Fig. 9A). Congo red staining of these GFAP-stained Aβ-exposed cultures showed that the plaques often were surrounded by several astrocytes (inserted picture in Fig. 9B). This finding is consistent with reports of activation of astrocytes surrounding beta-amyloid deposits (Domenici et al. 2002). Several cells with morphology resembling the microglial/macrophages were identified with the OX42 and ED1 antibodies. Brain macrophages have previously been shown to be ED1- and OX42-immunopositive, while microglia that are smaller, are OX42-positive and usually ED1-negative (Milligan et al. 1991). Although we could see a few affected OX42 and ED1 immunoreactive cells, most cells seemed unaffected following A$\beta_{25–35}$ exposure, a finding that is in line with previous in vitro studies, where no or very small microglial activation was demonstrated after exposure to A$\beta_{25–35}$. Specific domains of Aβ have been proposed to be necessary for microglial activation, including the non-toxic 10–16 region. Aβ peptides that contain the N-terminal, Aβ 1–28, bind to microglia, whereas the C-terminal portion of Aβ, Aβ 17–43, does not bind to microglia (Giulian et al. 1996). The lack of any obvious morphological changes in OX42 or ED1 labelled cells following A$\beta_{25–35}$ exposure may therefore be due to an inability of A$\beta_{25–35}$ to activate microglia.

The roller-drum hippocampal slice in vitro system of Aβ-induced toxicity, may serve as a useful model for studies on processes implicated in neurodegeneration. The cultures retain general cytoarchitecture of the in situ tissue while providing possibilities for in vitro studies bridging to in vivo systems. Different cell types characteristic of hippocampus were identified in the slice cultures, including pyramidal and GABA neurons, astrocytes and microglial cells, suggesting that key cellular phenotypes were retained in vitro. A$\beta_{25–35}$ exposure gave rise to fibrillar aggregates, showing classic staining characteristics of AD plaques, concomitant with neuronal degeneration of the pyramidal neurons. Also GABAegric interneurons stained with GAD 65 were damaged, while GABA-positive cells remained relatively unaffected following the Aβ exposure. Neurons immunopositive for phosphorylated tau epitopes showed degenerating and bent processes after Aβ exposure. GFAP positive astrocytes turned into a more reactive phenotype following A$\beta_{25–35}$ exposure, while OX42/ED1 positive microglia/macrophages seemed unaffected. This culture system containing several cell populations could therefore be used to study mechanisms of Aβ-induced neurodegeneration as well as to characterize neuroprotective approaches against Aβ-induced cell death.

Acknowledgements This work was supported by the Swedish Research Council (06537), the Swedish Heart and Lung Foundation, Alzheimerfonden, Gun and Bertil Stohnes stiftelse and Stiftelsen för Gamla Tjänarinnor.

References

Abe K, Saito H (2000) Amyloid beta neurotoxicity not mediated by the mitogen-activated protein kinase cascade in cultured rat hippocampal and cortical neurons. Neurosci Lett 292:1–4

Allen YS, Devanathan PH, Owen GP (1995) Neurotoxicity of beta-amyloid protein: cytochemical changes and apoptotic cell death investigated in organotypic cultures. Clin Exp Pharmacol Physiol 22:370–371

Andersson H, Luthman J, Olson L (1994) Trimethyltin-induced expression of GABA and vimentin immunoreactivities in astrocytes of the rat brain. Glia 11:378–382

Bamberger ME, Landreth GE (2002) Inflammation, apoptosis, and Alzheimer's disease. Neuroscientist 8:276–283

Beach RL, Bathgate SL, Cotman CW (1982) Identification of cell types in rat hippocampal slices maintained in organotypic cultures. Brain Res 255:3–20

Bobinski M, Wegiel J, Tarnawski M, de Leon MJ, Reisberg B, Miller DC, Wisniewski HM, (1998) Duration of neurofibrillary changes in the hippocampal pyramidal neurons. Brain Res 799:156–158

Braak H, Braak E, (1994) Morphological criteria for the recognition of Alzheimer's disease and the distribution pattern of cortical changes related to this disorder. Neurobiol Aging 15:355–356, 379–380

Buee-Scherrer V, Condamines O, Mourton-Gilles C, Jakes R, Goedert M, Pau B, Delacourte A (1996) AD2, a phosphorylation-dependent monoclonal antibody directed against tau proteins found in Alzheimer's disease. Brain Res Mol Brain Res 39:79–88

Burack MA, Halpain S (1996) Site-specific regulation of Alzheimer-like tau phosphorylation in living neurons. Neuroscience 72:167–184

Busciglio J, Lorenzo A, Yeh J, Yankner BA (1995) beta-amyloid fibrils induce tau phosphorylation and loss of microtubule binding. Neuron 14:879–888

Casal C, Serratosa J, Tusell JM (2002) Relationship between beta-AP peptide aggregation and microglial activation. Brain Res 928:76–84

Combs CK, Coleman PD, O'Banion MK (1998) Developmental regulation and PKC dependence of Alzheimer's-type tau phosphorylations in cultured fetal rat hippocampal neurons. Brain Res Dev Brain Res 107:143–158

Doig AJ, Hughes E, Burke RM, Su TJ, Heenan RK, Lu J (2002) Inhibition of toxicity and protofibril formation in the amyloid-beta peptide beta(25–35) using *N*-methylated derivatives. Biochem Soc Trans 30:537–542

Domenici MR, Paradisi S, Sacchetti B, Gaudi S, Balduzzi M, Bernardo A, Ajmone-Cat MA, Minghetti L, Malchiodi-Albedi F (2002) The presence of astrocytes enhances beta amyloid-induced neurotoxicity in hippocampal cell cultures. J Physiol Paris 96:313–316

Esclapez M, Tillakaratne NJ, Kaufman DL, Tobin AJ, Houser CR (1994) Comparative localization of two forms of glutamic acid decarboxylase and their mRNAs in rat brain supports the concept of functional differences between the forms. J Neurosci 14:1834–1855

Gähwiler BH (1981) Organotypic monolayer cultures of nervous tissue. J Neurosci Methods 4:329–342

Giulian D, Haverkamp LJ, Yu JH, Karshin W, Tom D, Li J, Kirkpatrick J, Kuo LM, Roher AE (1996) Specific domains of

beta-amyloid from Alzheimer plaque elicit neuron killing in human microglia. J Neurosci 16:6021–6037
Glenner GG (1989) The pathobiology of Alzheimer's disease. Annu Rev Med 40:45–51
Glenner GG, Wong CW (1984) Alzheimer's disease: initial report of the purification and characterization of a novel cerebrovascular amyloid protein. Biochem Biophys Res Commun 120:885–890
Goedert M, Jakes R, Crowther RA, Six J, Lubke U, Vandermeeren M, Cras P, Trojanowski JQ, Lee VM (1993) The abnormal phosphorylation of tau protein at Ser-202 in Alzheimer disease recapitulates phosphorylation during development. Proc Natl Acad Sci USA 90:5066–5070
Goedert M, Jakes R, Vanmechelen E (1995) Monoclonal antibody AT8 recognizes tau protein phosphorylated at both serine 202 and threonine 205. Neurosci Lett 189:167–170
Grundke-Iqbal I, Iqbal K, Quinlan M, Tung YC, Zaidi MS, Wisniewski HM (1986) Microtubule associated protein tau. A component of Alzheimer paired helical filaments. J Biol Chem 261:6084–6089
Hanger DP, Betts JC, Loviny TLF, Blackstock WP, Anderton BH (1998) New phosphorylation sites identified in hyperphosphorylated tau (paired helical filament-tau) from Alzheimer's disease brain using nanoelectronspray mass spectrometry. J Neurochem 71:2465–2476
Harrigan MR, Kunkel DD, Nguyen LB, Malouf AT (1995) Beta amyloid is neurotoxic in hippocampal slice cultures. Neurobiol Aging 16:779–789
Ikonomovic MD, Mizukami K, Warde D, Sheffield R, Hamilton R, Wenthold RJ, Armstrong DM (1999) Distribution of glutamate receptor subunit NMDAR1 in the hippocampus of normal elderly and patients with Alzheimer's disease. Exp Neurol 160:194–204
Klunk WE, Pettegrew JW, Abraham DJ (1989) Quantitative evaluation of congo red binding to amyloid-like proteins with a beta-pleated sheet conformation. J Histochem Cytochem 37:1273–1281
Klunk WE, Wang Y, Huang GF, Debnath ML, Holt DP, Mathis CA (2001) Uncharged thioflavin-T derivatives bind to amyloid-beta protein with high affinity and readily enter the brain. Life Sci 69:1471–1484
LeVine H III (1993) Thioflavine T interaction with synthetic Alzheimer's disease beta-amyloid peptides: detection of amyloid aggregation in solution. Protein Sci 2:404–410
Luthman J, Radesäter AC, Öberg C (1998) Effects of the 3-hydroxyanthranilic acid analogue NCR-631 on anoxia-, IL-1 beta- and LPS-induced hippocampal pyramidal cell loss in vitro. Amino Acids 14:263–269
Malouf AT (1992) Effect of beta amyloid peptides on neurons in hippocampal slice cultures. Neurobiol Aging 13:543–551
Milligan CE, Cunningham TJ, Levitt P (1991) Differential immunochemical markers reveal the normal distribution of brain macrophages and microglia in the developing rat brain. J Comp Neurol 314:125–135
Misonou H, Morishima-Kawashima M, Ihara Y (2000) Oxidative stress induces intracellular accumulation of amyloid beta-protein (Abeta) in human neuroblastoma cells. Biochemistry 39:6951–6959
Otvos L Jr, Feiner L, Lang E, Szendrei GI, Goedert M, Lee VM (1994) Monoclonal antibody PHF-1 recognizes tau protein phosphorylated at serine residues 396 and 404. J Neurosci Res 39:669–673
Pakaski M, Farkas Z, Kasa P Jr, Forgon M, Papp H, Zarandi M, Penke B, Kasa P Sr (1998) Vulnerability of small GABAergic neurons to human beta-amyloid pentapeptide. Brain Res 796:239–246
Perlmutter LS, Barron E, Chui HC (1990) Morphologic association between microglia and senile plaque amyloid in Alzheimer's disease. Neurosci Lett 119:32–36
Pike CJ, Cotman CW (1993) Cultured GABA-immunoreactive neurons are resistant to toxicity induced by beta-amyloid. Neuroscience 56:269–274
Pike CJ, Walencewicz AJ, Glabe CG, Cotman CW (1991) In vitro aging of beta-amyloid protein causes peptide aggregation and neurotoxicity. Brain Res 563:311–314
Pike CJ, Burdick D, Walencewicz AJ, Glabe CG, Cotman CW (1993) Neurodegeneration induced by beta-amyloid peptides in vitro: the role of peptide assembly state. J Neurosci 13:1676–1687
Pike CJ, Cummings BJ, Cotman CW (1995a) Early association of reactive astrocytes with senile plaques in Alzheimer's disease. Exp Neurol 132:172–179
Pike CJ, Walencewicz-Wasserman AJ, Kosmoski J, Cribbs DH, Glabe CG, Cotman CW (1995b) Structure-activity analyses of beta-amyloid peptides: contributions of the beta 25–35 region to aggregation and neurotoxicity. J Neurochem 64:253–265
Rapoport M, Dawson HN, Binder LI, Vitek MP, Ferreira A (2002) Tau is essential to beta -amyloid-induced neurotoxicity. Proc Natl Acad Sci USA 99:6364–6369
Sage BH Jr, O'Connell JP, Mercolino TJ (1983) A rapid, vital staining procedure for flow cytometric analysis of human reticulocytes. Cytometry 4:222–227
Schmued LC, Hopkins KJ (2000) Fluoro-Jade B: a high affinity fluorescent marker for the localization of neuronal degeneration. Brain Res 874(2):123–130
Schmued LC, Albertson C, Slikker W Jr (1997) Fluoro-Jade: a novel fluorochrome for the sensitive and reliable histochemical localization of neuronal degeneration. Brain Res 751:37–46
Selkoe DJ, Yamazaki T, Citron M, Podlisny MB, Koo EH, Teplow DB, Haass C (1996) The role of APP processing and trafficking pathways in the formation of amyloid beta-protein. Ann N Y Acad Sci 777:57–64
Sperk G, Schwarzer C, Tsunashima K, Fuchs K, Sieghart W (1997) $GABA_A$ receptor subunits in the rat hippocampus I: Immunocytochemical distribution of 13 subunits. Neuroscience 80:987–1000
Stoppini L, Buchs PA, Muller D (1991) A simple method for organotypic cultures of nervous tissue. J Neurosci Methods 37:173–182
Takashima A, Honda T, Yasutake K, Michel G, Murayama O, Murayama M, Ishiguro K, Yamaguchi H (1998) Activation of tau protein kinase I/glycogen synthase kinase-3beta by amyloid beta peptide (25–35) enhances phosphorylation of tau in hippocampal neurons. Neurosci Res 31:317–323
Toro VC, Tehranian R, Zetterstrom M, Eriksson G, Langel U, Bartfai T, Iverfeld K (2001) Increased gene expression of interleukin-1alpha and interleukin-6 in rat primary glial cells induced by beta-amyloid fragment. J Mol Neurosci 17:341–350
Yankner BA, Duffy LK, Kirschner DA (1990) Neurotrophic and neurotoxic effects of amyloid beta protein: reversal by tachykinin neuropeptides. Science 250:279–282
Zheng WH, Bastianetto S, Mennicken F, Ma W, Kar S (2002) Amyloid beta peptide induces tau phosphorylation and loss of cholinergic neurons in rat primary septal cultures. Neuroscience 115:201–211
Zimmer J, Gähwiler BH (1984) Cellular and connective organization of slice cultures of the rat hippocampus and fascia dentata. J Comp Neurol 228:432–446